Concussion Induces Hippocampal Circuitry Disruption in Swine

John A. Wolf,[1,2] Brian N. Johnson,[3] Victoria E. Johnson,[1] Mary E. Putt,[4] Kevin D. Browne,[1,2]
Constance J. Mietus,[1] Daniel P. Brown,[1,2] Kathryn L. Wofford,[1,2] Douglas H. Smith,[1]
M. Sean Grady,[1] Akiva S. Cohen,[3] and D. Kacy Cullen[1,2]

Abstract

Hippocampal-dependent deficits in learning and memory formation are a prominent feature of traumatic brain injury (TBI); however, the role of the hippocampus in cognitive dysfunction after concussion (mild TBI) is unknown. We therefore investigated functional and structural changes in the swine hippocampus following TBI using a model of head rotational acceleration that closely replicates the biomechanics and neuropathology of closed-head TBI in humans. We examined neurophysiological changes using a novel *ex vivo* hippocampal slice paradigm with extracellular stimulation and recording in the dentate gyrus and CA1 occurring at 7 days following non-impact inertial TBI in swine. Hippocampal neurophysiology post-injury revealed reduced axonal function, synaptic dysfunction, and regional hyperexcitability at one week following even "mild" injury levels. Moreover, these neurophysiological changes occurred in the apparent absence of intra-hippocampal neuronal or axonal degeneration. Input–output curves demonstrated an elevated excitatory post-synaptic potential (EPSP) output for a given fiber volley input in injured versus sham animals, suggesting a form of homeostatic plasticity that manifested as a compensatory response to decreased axonal function in post-synaptic regions. These data indicate that closed-head rotational acceleration–induced TBI, the common cause of concussion in humans, may induce significant alterations in hippocampal circuitry function that have not resolved at 7 days post-injury. This circuitry dysfunction may underlie some of the post-concussion symptomatology associated with the hippocampus, such as post-traumatic amnesia and ongoing cognitive deficits.

Keywords: axonal pathology; concussion; epileptogenesis; hippocampus; mild TBI; traumatic brain injury

Introduction

MILD TRAUMATIC BRAIN INJURY (MTBI), also known as concussion, has been recognized as a major health issue due to heightened awareness of sports-related brain injuries and the prevalence of mTBI in contemporary military conflicts.[1–4] This injury is by no means "mild," considering that many individuals suffer persistent neurocognitive dysfunction, including post-traumatic amnesia.[5,6] Recent reports have suggested that even a single mTBI can potentially lead to long-term neuroradiological and behavioral consequences.[7] Moreover, mTBI can cause structural changes to axons in the white matter in some clinical cases and in animal models.[8,9] However, the mechanisms underlying the early symptomatology, such as post-traumatic amnesia and deficits in information processing following mTBI, have remained obscure.

In moderate-to-severe TBI in humans, the hippocampus has been shown to be selectively vulnerable, with demonstrable neuronal degeneration.[10,11] The hippocampus also has drawn widespread attention due to its selective vulnerability and changes in excitability after a range of mechanical perturbations in rodent models of TBI.[12–16] However, neuronal degeneration does not appear to be a typical feature of mTBI,[8,9] raising the possibility that cognitive deficits are due to network circuitry dysfunction rather than resulting from overt neurodegeneration.

In the current study, our objective was to investigate structural and functional alterations in hippocampal circuitry following diffuse brain injury. We therefore utilized an established swine model of diffuse brain injury induced by non-impact closed-head rotation[17–19] that has recently been adapted to replicate mechanical loading conditions comparable to those found in human mTBI.[8] To

[1]Department of Neurosurgery, [4]Department of Biostatistics and Epidemiology, Perelman School of Medicine, University of Pennsylvania, Philadelphia, Pennsylvania.
[2]Center for Neurotrauma, Neurodegeneration, and Restoration, Corporal Michael J. Crescenz Veterans Affairs Medical Center, Philadelphia, Pennsylvania.
[3]Department of Anesthesiology and Critical Care Medicine, Children's Hospital of Philadelphia, Philadelphia, Pennsylvania.

isolate hippocampal function, we developed a hippocampal slice paradigm for swine and utilized it to examine axonal conduction, synaptic function, and neuronal excitability to stimulation in area CA1 and the dentate gyrus following rotational head injury. We found that hippocampal neurophysiology was profoundly affected following mTBI, including reduced axonal function, synaptic dysfunction, and regional hyperexcitability. Moreover, these neurophysiological changes did not appear to correlate with intra-hippocampal neuronal or axonal degeneration. To the best of our knowledge, this is the first reported electrophysiological examination of the hippocampus following diffuse brain injury in a gyrencephalic large mammal. These findings suggest that hippocampal circuitry dysfunction may be an important aspect of mTBI, and may underlie or contribute to post-traumatic cognitive deficits.

Methods

Animal preparation

Female 2- to 3-month-old Yorkshire swine ($N = 12$) with an average weight of 24.3 kg were utilized in this study. The animals were housed indoors and were fed standard pig chow and water *ad libitum.* The animals were housed in a facility that was accredited by the Association for Assessment and Accreditation of Laboratory Animal Care International. The protocol was approved by the Animal Care and Use Committee of the University of Pennsylvania and all animals received care in strict compliance with the Guide for the Care and Use of Laboratory Animals (U.S. National Research Council, 1996).

Closed-head rotation induced diffuse brain injury using the HYGE pneumatic actuator. Animals were fasted for 18–20 h prior to the injury procedure, with water allowed *ad libitum.* After pre-medication with midazolam (4.0–6.0 mg/kg), anesthesia was induced with 5% isoflurane by snout mask, followed by intubation and isoflurane at maintenance levels (1.5–2.0%). Closed-head rotational acceleration-deceleration–induced TBI was administered using the HYGE pneumatic actuator, a model capable of producing pure impulsive non-impact head rotation in different planes (Fig. 1) at controlled rotational acceleration levels (thus controlling severity).[17–19] Briefly, under anesthesia, the animals' heads were secured to a padded snout clamp, which, in turn, was mounted to the HYGE device using a custom linkage assembly that converts the linear motion of the actuator to an angular (rotational) motion. Rapid head rotation was performed in the coronal plane at peak angular velocities of 131–195 radians/sec ($n = 7$). Sham animals received all ancillary procedures absent head rotation ($n = 5$). All animals were transported back to the animal facility for recovery and were survived for a period of 7 days.

Temporal lobectomy and hippocampal dissection

At 7 days post-TBI (or sham procedures), animals were induced with midazolam (2.5–3.0 mg/kg) combined with ketamine (6.0–8.0 mg/kg), intubated, and maintained on isoflurane as above (1.5–2.0%). Animals were then transferred to a surgical suite where a craniotomy was performed to expose the entire surface of the cerebral cortex, and the dura was resected. The heart was accessed and a transcardial perfusion was performed initially using a sucrose artificial cerebrospinal fluid (aCSF; 3 mM KCl, 2.5 mM NaH$_2$PO$_4$, 26 mM NaHCO$_3$, 10 mM glucose, 1 mM MgCl$_2$, 2 mM CaCl$_2$, with sucrose replacing Na+ to match CSF osmolarity) chilled to 4°C. The left posterior quadrant of the brain was extracted using a scalpel (Fig. 1), and the remainder of the brain was then immediately transcardially perfused with 4% paraformaldehyde fixation for histopathological analysis of the contralateral hemisphere. The

live extracted tissue (prior to paraformaldehyde administration) was dissected on a cold block to isolate the hippocampal formation.

### Hippocampal slice acquisition and field potential recordings

Sham animals ($n = 2$) and injured animals ($n = 1$) were utilized in an initial study to develop the extraction and pathway stimulation and recording paradigms. Recordings in response to all stimulation paradigms in the study were obtained following sham conditions ($n = 3$ animals) and following coronal plane rotation ($n = 5$ animals) with $n = 4$–8 hippocampal slices assessed per animal. One animal rotated in the coronal plane was utilized for histopathology only ($n = 1$). For hippocampal slice electrophysiology, the extracted hippocampus was blocked to a 1-cm section transverse to the long axis, affixed to a vibratome stage (Leica, VT1200S), and cut to a thickness of 350 μm in ice-cold (2°C) oxygenated aCSF (5% CO$_2$, 95% O$_2$) with sucrose replacing NaCl to equal osmolarity (see above). Slices were then incubated in oxygenated aCSF (130 mM NaCl, 3 mM KCl, 1.25 mM NaH$_2$PO$_4$, 26 mM NaHCO$_3$, 10 mM glucose, 1 mM MgCl$_2$, 2 mM CaCl$_2$) at 35°C for 1 h.

Recordings were performed at room temperature on an interface chamber using glass electrodes (3–4 MOhm) filled with aCSF and an AxoPatch 1D amplifier in current clamp mode (Molecular Devices, CA). Slices were continuously perfused with oxygenated aCSF. Traces were digitized and analyzed using the PClamp 10.0 software package (Molecular Devices, CA). Recordings were performed in area CA1 while stimulating the Schaffer collaterals, and in the dentate while stimulating either the medial or lateral perforant path of the dorsal blade of the dentate gyrus. Care was taken to utilize the same distances between stimulating and recording electrodes ($\sim$2 mm), as well as between the medial and lateral perforant path.

Preliminary experiments revealed a waveform similar to previously reported rodent results in area CA1 that had a prominent fiber volley (FV) and field EPSP (Fig. 1). To confirm the waveform constituents, the EPSP was blocked with glutamatergic antagonists (APV, 50 μM, CNQX, 6 μM), after which the FV was completely blocked by the application of tetrodotoxin (TTX) (0.4 μM; data not shown), leaving only the stimulation artifact (removed for clarity in all presented traces). Input–output (I/O) curves were generated and paired-pulse paradigms were utilized to examine changes in excitability and neurotransmitter release probabilities in slices from injured versus sham animals. Stimulation was applied with a concentric bipolar stimulating electrode in the range of 50–500 μA. The stimulation current eliciting half of the maximal I/O response was determined, and two pulses at this current level were then given 50 ms apart for the paired-pulse paradigm. This paired-pulse paradigm was repeated 10 times with a 10 sec interval between trials. To calculate paired-pulse facilitation or depression, the linear portion of the second EPSP slope (approximately 75% of the deflection) was compared to the first EPSP slope, utilizing the same time window relevant to the stimulus artifact for both pulses. FV slopes were calculated using the linear portion of the initial negative deflection that was sensitive to TTX in initial experiments. I/O curves were initially generated using standard methodology with stimulation current as the input, but also were calculated using the measured FV slope as the input compared with the EPSP "output." These procedures were used for CA1 inputs from the Schaffer collaterals and for the dentate gyrus inputs from the perforant path, at both the medial and lateral portion of the dorsal blade of the gyrus.

Statistical analysis

The experimental design for these studies was a variation on a split-plot design, and therefore data were analyzed using analysis
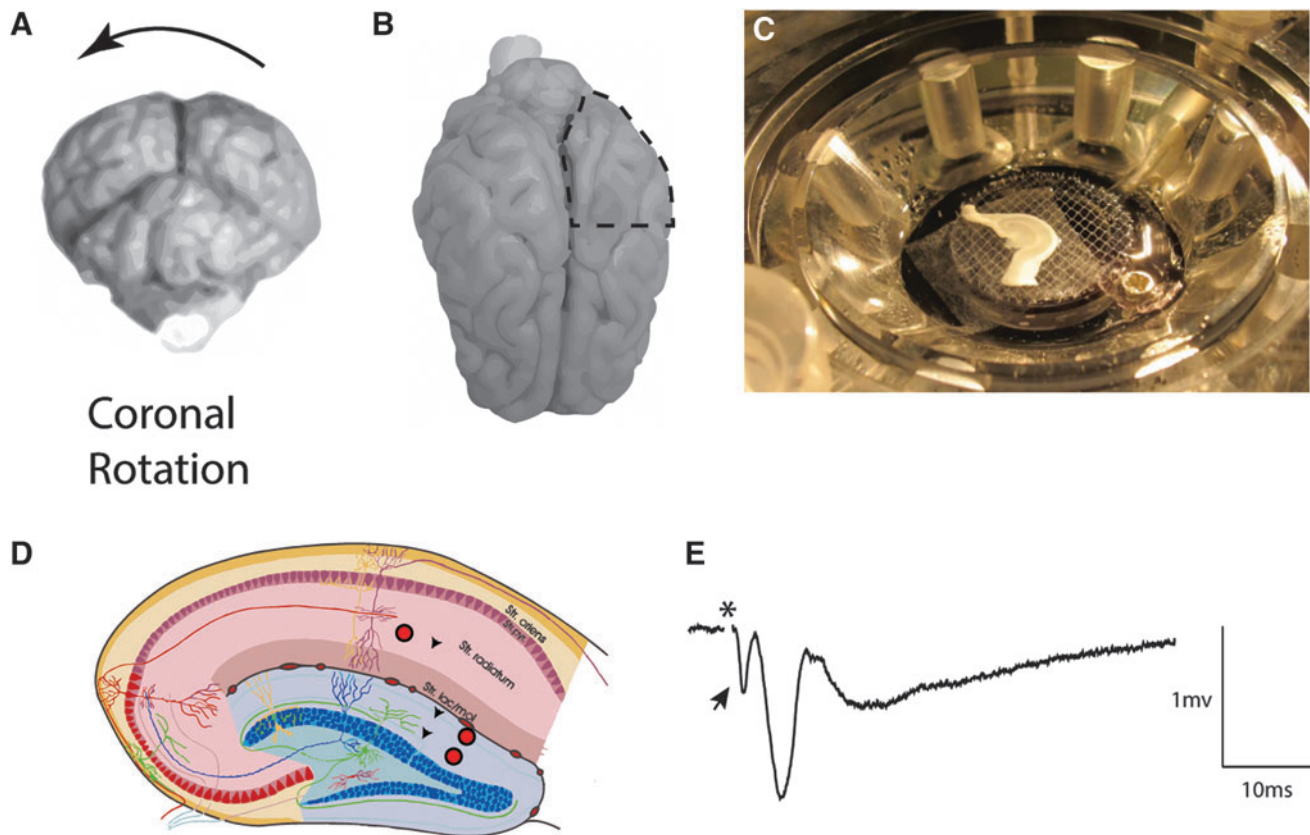
FIG. 1. Hippocampal slice recordings following rotational TBI in swine. Closed-head diffuse brain injury was induced based on rapid rotational acceleration-deceleration in the coronal plane as depicted in **(A)**. At terminal time-points of 7 days post-injury, pigs were transcardially perfused with cold, oxygenated artificial cerebrospinal fluid, the posterior left quadrant of the brain was removed **(B)**, and the remainder of the brain was fixed with paraformaldehyde. The live posterior quadrant was immediately dissected on a cold block, and the hippocampus was removed and blocked transversely to the long axis. Approximately 1cm of the dorsal hippocampus was then transferred to sucrose cutting solution (see Methods) and then $350\,\mu$M sections were cut on a vibratome. These sections were transferred to an interface chamber **(C)**, where stimulation (red circles) and recordings (black arrows) **(D)** were performed in the Schaffer collaterals (CA1) and the medial and lateral perforant path (dentate). A typical trace from CA1 **(E)** had a prominent fiber volley (FV) (arrow) immediately following the stimulation (artifact removed, *) followed by an excitatory post-synaptic potential (EPSP). (D) Modified from http://anatomie.vetmed.uni-leipzig.de/external/hippocampus/hippocampus_schema_gross.jpg

of variance (ANOVA) with two fixed factors, using the principles outlined in Morris.[20] An interaction term was included between the two factors in each ANOVA. A variation on this approach that included FV slope as a continuous variable was used for the analysis of the EPSP data.

All statistical models considered animals to be independent experimental units. Animal was modeled as a random effect; thus, we consider the animals in our study to represent a random sample of the population of animals under consideration. Within each animal, replicate slices were collected. These slices were assumed to be correlated within animals; they were not assumed to be independent units of analysis. Thus, two separate covariance terms were included in the statistical model: one for the repeated measurements on the same slice within animal, and one for repeated measurements on different slices within animals. Operationally, we carried this out by including a separate random term, nested within animal in our statistical model. An example of the implementation of this model is included in the supplementary Figure S1. Recording time post-extraction was not examined as a factor in this analysis.

The general hypothesis-testing strategy involved first applying ANOVA to test for the main effect of injury and the interaction between injury and either current or region; if this indicated sta-

tistical significance, individual effects were examined using Wald tests and estimates presented with 95% confidence intervals. The outcome data were log transformed to achieve approximate normality (with estimates exponentiated to return to the original scale).

Four separate statistical analyses were performed. First, for the paired pulse experiments, the factors in the ANOVA included injury group (injury present or absent) and brain region (CA1, medial perforant path [mPP], lateral perforant path [lPP]), and their interaction. The ratio of the slope of the EPSP for pulse 2 and pulse 1 was used as the outcome (results of this analysis shown in Fig. 3). Second, in order to assess mean differences in FV between injured and sham animals, the factors in the ANOVA were injury group and current (10 levels applied to each brain slice within each animal), and their interaction (Fig. 4). Third, we considered differences in mean EPSP as a function of injury group and current, using an analysis that followed the same protocol as described above where we considered differences in mean FV slope (Fig. 5A). The relationship between current and FV slope was visualized by determining the following: 1) the mean FV slope across slices (4 to 8 per animal) for each animal and 2) the mean of the mean FV slope determined across animals. This was done at each current level. Lastly, we considered whether mean EPSP differed as a function of FV slope between sham and injured animals. We plotted these data

in two ways. To present the data in a previously described manner, we first plotted the data using the mean EPSP as a function of the mean FV slope at each current level (Fig. 5B). We then used a mixed effects model to ask whether mean EPSP differed as a function of injury group and FV slope. Thus, the fixed effects factors in this statistical model were injury group, FV slope, and their interaction. The model also included current since mean EPSP was shown to increase with current for the ranges examined.

FV slope was modeled statistically using a cubic spline; this is a simple approach to allowing a curvilinear model without specifying a particular parametric form. Of particular interest was the interaction between injury group and FV slope; presence of a significant interaction would suggest that the effect of injury was dependent on the magnitude of the FV slope. This model is similar to the analysis we used to test the effect of current on FV slope. Here, instead of a current by injury interaction, we anticipated a FV slope by injury interaction. The second plot (supplementary Fig. S1) was used to simply visualize the results of this model. As such, we plotted the estimated mean EPSP as a function of FV slope for each current and each injury group. We did this for each brain region. For simplicity, we plot only the mean function; these results should be considered hypothesis generating and are intended to supplement our main finding which were based on more traditional analytic approaches (Fig. 5B). For all I/O and FV curves, the standard error of the mean (SEM) was calculated based on the variation in the means for each animal ($n = 3$ sham or $n = 5$ injured). We used two-sided tests and a Type I error rate of 0.05. Analyses were carried out in R Studio Version 0.99.467 using R (R Core Team 2016) version 3.3.0 and the nlme package.[21]

Immunohistochemistry

Brain hemispheres (contralateral to the live-tissue excision) were blocked into coronal sections at 0.5 cm intervals for gross examination and photography. All tissue samples were processed in paraffin using standardized protocols. Paraffin blocks containing the temporal lobe, including the hippocampal formation, were sectioned at 8 μm and mounted on glass slides. Immunohistochemistry was performed using techniques as previously described.[22] Briefly, following deparaffinization and rehydration, sections were immersed in aqueous hydrogen peroxide (10 min) to quench endogenous peroxidase activity. Antigen retrieval was performed in a microwave pressure cooker containing TRIS EDTA buffer and subsequent blocking achieved using 50 μL of normal horse serum (Vector Labs, Burlingame, CA) per 5 mL of Optimax buffer (BioGenex, San Ramon, CA) for 30 min. Incubation with the primary antibody was performed for 20 h at 4°C. Specifically, monoclonal antibodies specific for the heavy subunit of neurofilament (NF-200; N-0142; Sigma-Aldrich, St Louis, MO) and the N-terminal amino acids 66–81 of the amyloid precursor protein (APP; 22C11, Millipore, Billerica, MA) were applied at a concentration of 1:2 K and 1:50 K, respectively, to permit detection of axons and axonal pathology.[23–26] A biotinylated universal secondary antibody was then applied for 1 h (Vectastain Universal Elite kit; Vector Labs, Burlingame, CA) followed by an avidin biotin complex as per the manufacturer's instructions (Vectastain Universal Elite kit).

Finally, visualization was achieved using the DAB peroxidase substrate kit (Vector Labs, Burlingame, CA). Counterstaining with hematoxylin was performed and sections were examined using light microscopy on a Nikon E600 eclipse and images acquired via a Nikon RI1 camera. Positive control tissue included identically prepared tissue from swine exposed to higher level coronal rotational acceleration (280 radians/sec) using the same model, with previously confirmed axonal pathology. Omission of the primary antibody was performed on the same material to control for non-specific binding. In all animals, the presence, morphology, and distribution of axonal pathology was assessed in the temporal lobe including regions relative to electrophysiological findings, specif-

ically the stratum moleculare layer of the dentate gyrus and the stratum radiatum of the CA1 region of the hippocampus. Observations were conducted blind to the injury status by two independent observers (V.E.J. and J.A.W.).

Results

Neurological recovery and gross pathology

We used an established swine TBI model based on head rotational acceleration at peak angular velocities shown to induce specific patterns and distributions of pathology.[18,27] Swine were rotated in the coronal plane, while sham animals received equivalent procedures absent head rotation. Swine undergoing rotational injury had no post-injury loss of consciousness and recovery was indistinguishable from anesthesia effects in sham animals; ambulation was restored soon after withdrawal of inhalation anesthesia and the animals began feeding within a few hours. Gross examination of brains from swine undergoing head rotation revealed no gross evidence of other TBI-related focal pathology, hematoma, mid-line shift, or herniation. Overall, rotation in the coronal plane was consistent with mTBI as previously demonstrated.[27–29]

Changes in hippocampal electrophysiology post-TBI

We developed a hippocampal slice preparation for swine in order to investigate neurophysiological changes post-injury (see Methods; Fig. 1). Hippocampal slice recordings demonstrated overt changes in the waveforms of the extracellular post-synaptic responses to afferent stimulation in both area CA1 and dentate gyrus post-injury during stimulation of the Schaffer collaterals and the perforant path (medial and lateral), respectively. These changes, which appear to be an invasion of single or multiple population spikes earlier in the waveform and are believed to be summed action potentials from the cell layer, were most prominent in area CA1 (Fig. 2). Changes in the dentate response waveforms following stimulation of the perforant path were less consistent following TBI, as invasion of the population spike was only present in a subset of animals when stimulated in the medial perforant path. Moreover, changes in response waveforms were not apparent when stimulated and recorded in the lateral perforant path, presumably due to the increased distance of the dentate granule neurons from the recording electrode. These alterations, when present, suggest increased network excitability, a shift in the excitation–inhibition balance of the local circuitry, or a potential homeostatic increase in synaptic current leading to hyper-responsiveness.

I/O curves were generated based on stimulation between 50 and 500 μA of current, and the half maximal response was utilized for a paired-pulse paradigm to investigate changes in synaptic function. Examination of paired pulse facilitation at 50 msec intervals revealed potential changes in neurotransmitter release probabilities from injured versus sham animals. In area CA1, paired pulse facilitation was evident in the sham condition, as has been demonstrated in other species.[30] However, we found a loss of this paired pulse facilitation post-injury in area CA1 ($p = 0.006$; Fig. 3). This decrease in paired-pulse facilitation post-injury suggests that there may be an increase in release probability at 7 days post-injury. In contrast, in the dentate gyrus, a trend towards paired pulse depression in the medial perforant path and a trend towards facilitation in the lateral perforant path were evident in sham animals as has been reported in the rodent,[31] but these were not significantly different following injury ($p = 0.18$ and $p = 0.097$ in the mPP and lPP, respectively; Fig. 3).
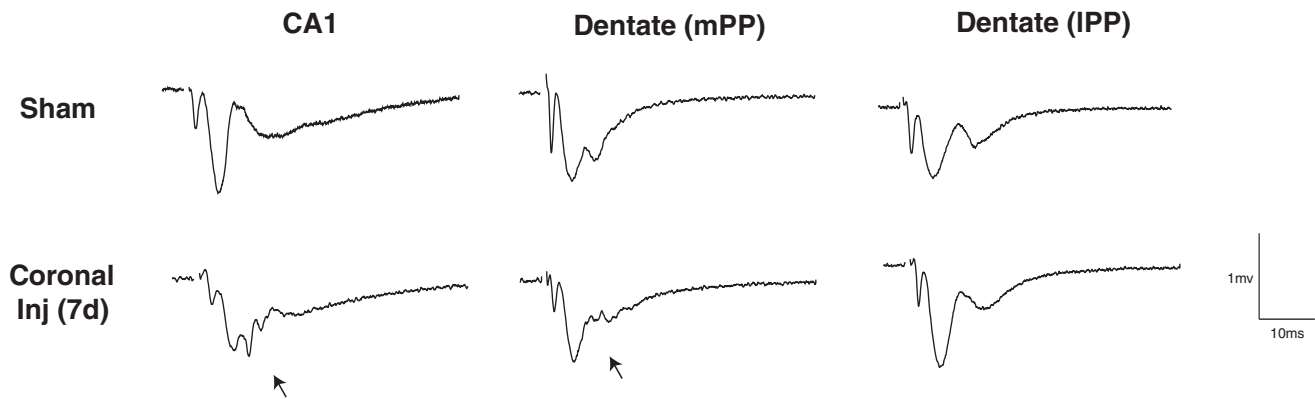
FIG. 2. Changes in response waveform post-TBI in area CA1 and dentate gyrus. Representative examples of responses to stimuli in the Schaffer collaterals (CA1) or medial perforant path (mPP) and lateral performant path (lPP) in hippocampal slices after rotational brain injury in swine. Each waveform is the average of 10 traces at the half-maximal stimulation. Note the profound disruption in the EPSP post-injury in area CA1 and in the dentate when stimulating the mPP (arrows). A distinct pattern commonly appears in the waveforms post-injury that may be due to the population activity response invading the EPSP, suggesting hyper-excitability in the neuronal response.

We also assessed TBI-induced changes in intra-hippocampal FVs via extracellular recordings of presynaptic action potentials induced by stimulation (same stimulation/recording positions as above). We observed a prominent FV in the sham pig hippocampal slices, and a notable decrease in the FV was evident in many cases post-injury. When quantified, we found significant decreases in mean FV initial slope following TBI (Fig. 4). Specifically, in area CA1, we found overall decreases in FV slope for injured versus sham animals. The injured group on average had mean FVs that were 52% of the sham ($p = 0.028$). In both perforant pathways analyzed, mean FVs were lower in injured, compared with sham animals; however, these results were not statistically significant, and there appeared to be greater variability in FVs in these pathways, compared with the Schaffer collaterals.

Interestingly, conventional I/O curves (based on stimulation current versus EPSP) were similar between injured and sham animals at these stimulation levels (Fig. 5A). However, as described above, the FVs were substantially reduced in CA1 post-injury. Therefore, in order to visualize the potential effect of diminished FV inputs, we plotted the EPSP slope against the mean FVs as has previously been described (Fig. 5B).[32–34] Accordingly, we analyzed the EPSP output based on FV inputs at each current level in order to address whether the relationship between EPSP and FV slope differed between injured and sham animals. For CA1, this analysis showed that EPSP was significantly higher as a function of FV slope among the injured animals than among sham animals ($p = 0.001$), although the ratio between these was smaller at lower FV slopes. In addition, there was an effect of current on this interaction in area CA1, such that there were greater differences at higher current levels (Fig. S1). Taken together, our results support the hypothesis that in CA1, the relationship between axonal ''input'' and the synaptic currents measured in the EPSP suggests a compensatory response to the lower FV post-TBI, as demonstrated by the change in this relationship post injury in CA1.

Intra- and extra-hippocampal neuropathology

We hypothesized that the observed reduction in intra-hippocampal FVs may be explained by a concomitant reduction in axonal density from diffuse axonal injury and degeneration. To examine for this, we performed APP immunohistochemistry in tissue sections containing the hippocampus as well as the temporal lobe white matter. APP immunoreactive axons displayed the classic morphological appearance of traumatic axonal injury, including terminally disconnected swollen axonal bulbs (formerly referred to as retraction balls), and varicose swellings along the length of intact axons.[23–25,35] Nominal axonal pathology was observed in multiple areas of the white matter tracts of the temporal lobe following coronal rotation at 7 days post-injury (Fig. 6B). Although minimal in extent, the morphological appearance of the extra-hippocampal axonal pathology was consistent with that previously observed in this model.[17,18,36] Notably, no overt APP accumulation was observed within the hippocampal formation in any animals, including regions that directly corresponded to the stimulation and recording sites of the hippocampus on the alternate hemisphere. Specifically, axons in the stratum moleculare layer of the dentate gyrus and the stratum radiatum of the CA1 did not exhibit APP accumulation post-TBI (Fig. 6D, 6F). Since APP is a marker of ongoing transport interruption, we cannot exclude the possibility that axons degenerated outside the time-points examined. However, as a previously identified marker of all axons,[26] NF-200 revealed axons with a density, morphology, and distribution in these regions indistinguishable from controls, with no overt evidence of axonal dropout (Fig. 6H, 6J), although this staining does not rule out more subtle changes in NF expression or distribution. Hematoxylin and eosin staining (data not shown) revealed a small number of ''dark'' neurons in the hippocampal structure at equal levels in sham and injured animals, most likely an artifact of the surgical resection of the temporal lobe.

Discussion

The vast majority of TBIs are closed-head diffuse brain injuries caused by inertial loading to the head.[28,36–40] Even so-called ''mild'' TBI (concussion) can lead to significant cognitive disruption, which may or may not include loss of consciousness immediately post-injury, as well as longer-term neurological deficits such as deficits in short-term memory and cognitive processing.[41–44] These initial disruptions in short-term memory and cognition are

A

B

CA1

C

Dentate (mPP)

D

Dentate (lPP)
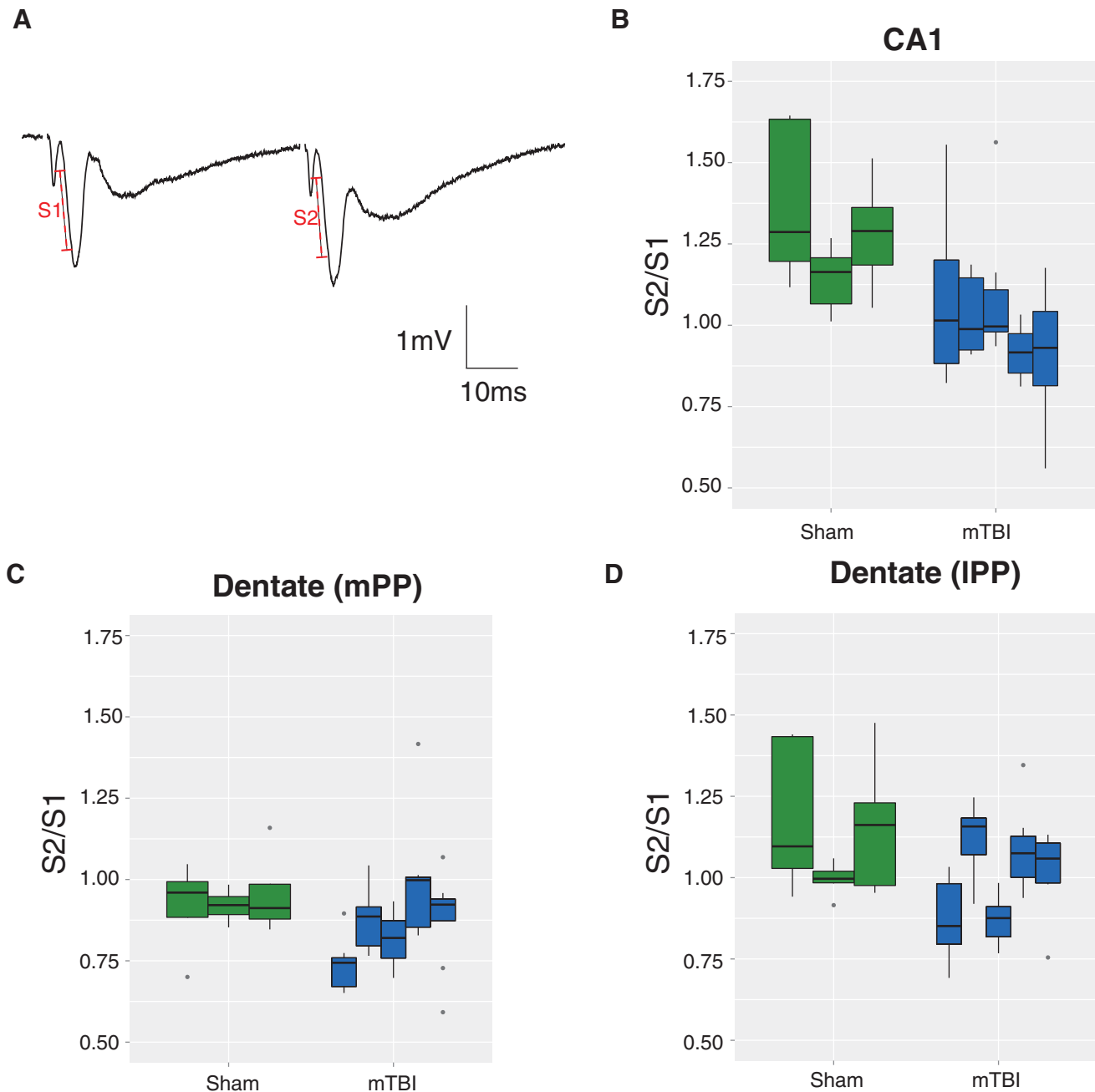
FIG. 3. Changes in paired pulse facilitation and depression post-TBI. **(A)** Paired pulse facilitation (PPF) as demonstrated in area CA1, where an increased slope (S2) was evident in the second pulse (50 msec interpulse interval). An analysis of variance including injury group and an interaction with brain region yielded evidence of a significant main effect of injury [$F_{(1,6)} = 11.5$, $p = 0.015$], as well as evidence of differences in the effect of injury in the three different brain regions [$F_{(2,98)} = 3.29$, $p = 0.042$]. **(B)** Compared with sham, recordings in area CA1 suggested PPF was reduced by a factor of 0.79 (95% CI 0.69, 0.91; $p = 0.006$] following mild head rotation. **(C)** Responses to stimulation in the dentate (medial perforant path [mPP]) suggested injured animals showed a reduction of 0.91-fold (95% CI 0.80, 1.05) relative to sham animals ($p = 0.18$). **(D)** Similar PPF occurred in sham recordings in the lateral perforant path (lPP), with a reduction of 0.90-fold (95% CI 0.78, 1.03) in injured versus sham animals ($p = 0.097$). Note that these results for mPP and lPP did not achieve statistical significance. To visualize both between animal variation as well as within-animal variation arising from the multiple slices, the data are presented as boxplots for each individual animal; the horizontal line is the median, the box is the interquartile range (IQR) and each vertical line is the box ±1.5 IQR truncated at the minimum and maximum values for each animal. Outliers are shown as individual points.

suggestive of hippocampal dysfunction, as is post-traumatic amnesia.[43] Indeed, even a single mTBI can lead to long-term changes in both memory function and hippocampal structure.[7] The objective of the current study was to assess alterations in hippocampal circuitry as a potential substrate for this dysfunction using a well-

characterized swine model of closed-head rotational acceleration induced TBI. In order to examine electrophysiological changes in hippocampal circuitry post-injury, we developed methodology for slice recordings from the swine hippocampus. The data presented here suggest that closed-head diffuse brain injury leads to changes
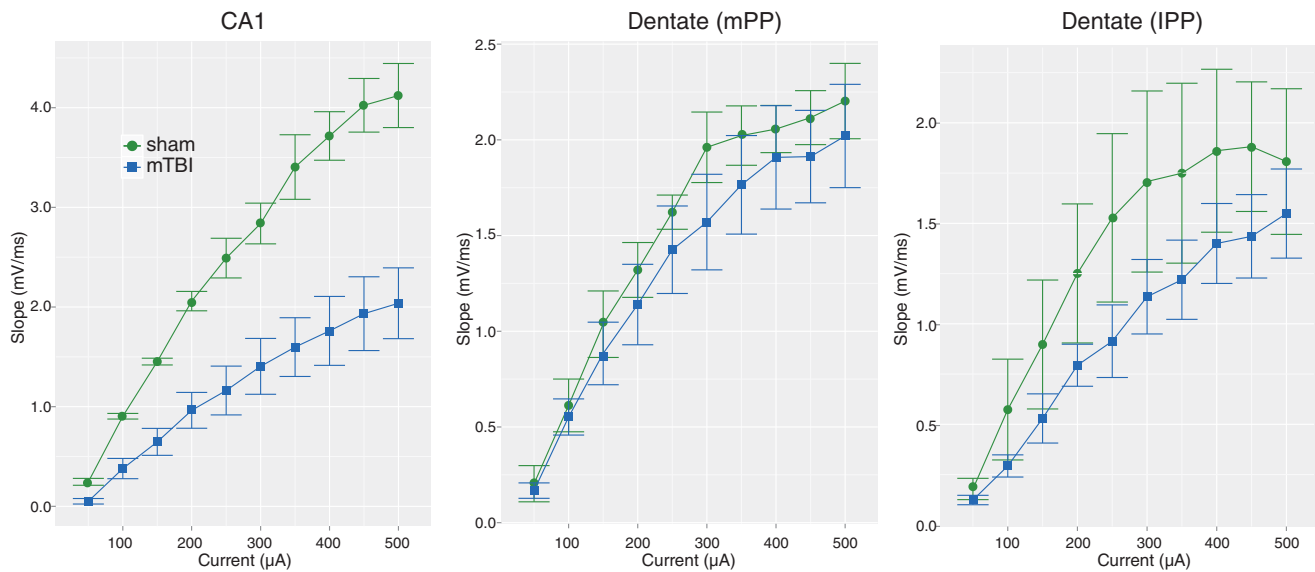
FIG. 4. Decrease in fiber volleys in CA1 at 7 days following mTBI. On average fiber volley slope in area CA1 was a factor of 0.52-fold (95% CI 0.47, 0.93) lower post-injury than sham (F(1,6) 0 = 8.3, $p < 0.028$), with no evidence of an injury interaction with current [F(9, 421) = 0.78, $p = 0.63$]. In region medial perforant path (mPP), the mean fiber volley slope of injured animals was a factor of 0.90-fold (95% CI 0.66, 1.313), compared with sham, [F(1,6) = 0.27, $p = 0.62$, NS for the main effect and F(9, 432) = 0.38, $p = 0.95$, NS for the interaction]. In region lPP fiber volley slope was a factor of 0.66-fold (95% CI 0.58, 1.19) lower post-injury than sham [F(1,6) = 4.67, $p = 0.25$ and F(9, 432) = 1.72, $p = 0.083$ for the interaction] but also not significant. Data shown are empirical means ± standard error of the mean (SEM) where the SEM is based on the number of animals per group.

in intra-hippocampal axonal conduction, synaptic function, and regional excitability at 1 week post-injury.

### Hippocampal excitability and homeostatic plasticity

One of the surprising results of this study was the presumed compensation for diminished input and resultant hyperexcitability present in area CA1 at 1 week post-injury. The invasion of the population spike was dramatic and in some cases created multiple population action potentials (''spikes''), suggesting overwhelmed inhibitory circuitry and/or hyperexcitable neurons as has been previously demonstrated in rodent models of epilepsy and after TBI in hippocampus and cortex.[32,45–47] Interestingly, overall I/O curves based purely on stimulation current amplitude and field EPSP slopes were not significantly different between sham and injured animals. However, when normalized to afferent FV amplitude instead of the stimulus intensity, the ''output'' was significantly greater in the injured animals, most prominently in area CA1. In combination with the overall decrease in FV levels, this suggests that there may be a compensatory change in the synapses of the CA1 neurons, leading to a greater response to each input. This homeostatic mechanism was first demonstrated in *in vitro* systems where reduction in afferent input lead to changes in intrinsic excitability and post-synaptic compensatory mechanisms.[48] This concept also has been previously demonstrated explicitly in the hippocampus by deafferentation of area CA1 via Schaffer collateral transection.[49] After transection, multiple population spikes were present in area CA1 following stimulation, although GABAergic systems did not appear to be disrupted. Also supporting this conclusion is the increase in dendritic spine size in area CA1 after fluid percussion injury in mice.[50] Our results suggest a homeostatic mechanism whereby decreasing input from afferent areas due to decreased axonal function leads to hyperexcitability in the post-synaptic neurons, although pre- or post-synaptic changes could be

responsible. Hyperexcitability in CA1 and dentate have previously been demonstrated in various rodent models, although the results vary depending on investigator and model utilized.[32,33,45,51,52]

Loss of hippocampal FVs and axonal pathology

Diffuse axonal injury has been demonstrated as one of the most important pathologies following closed-head TBI in humans and in animal models.[18,37–39,53] Whether TBI-induced axonal dysfunction beneath the level of axonal degeneration underlies cognitive dysfunction remains an open question. We therefore investigated intra- and extra-hippocampal axonal pathology based on APP immunoreactivity, a marker of transport interruption useful to morphologically identify axonal retraction bulbs and/or varicosities, which is the current gold standard for the clinical detection of axonal pathology.[23–25,35] This analysis revealed axonal pathology within sub-cortical white matter, as previously reported in this model.[18] However, no axonal pathology was observed in the regions where stimulations and recordings were performed (in the contralateral hemisphere) or at any location within the main hippocampal structure. Moreover, neurofilament staining revealed axonal tracts with normal morphology that appeared indistinguishable from uninjured controls.

However, a lack of hippocampal APP accumulation does not completely exclude the possibility of axonal pathology as a potential mechanism underlying electrophysiological changes, but rather may reflect the limitations of APP immunohistochemistry in detecting the entire population of injured axons. Specifically, APP immunohistochemistry relies upon the detection of abnormally accumulating APP in swollen or varicose axons as a consequence of interruption to axonal transport. As such, it remains possible that axons with intact transport that are otherwise functionally impaired would not be detected using this marker. Although it is also possible that hippocampal axonal degeneration had occurred outside the time-points at
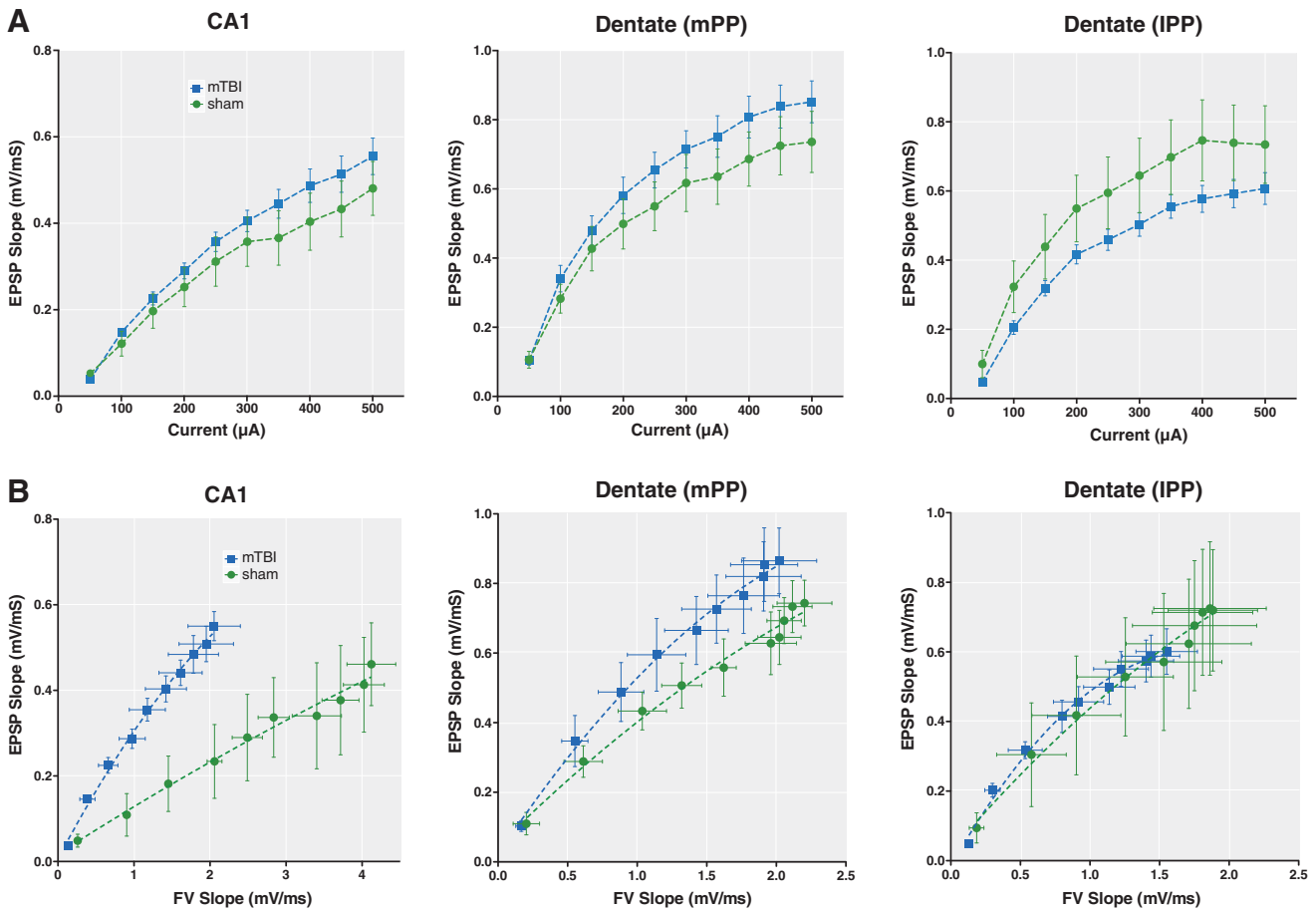
FIG. 5. Post-TBI output (EPSP) levels as a function of input (FV slope). **(A)** Input/output curves were generated via stimulation of the Schaffer collaterals and medial and lateral perforant path in the dentate region. The injured group trended towards higher mean EPSP levels in CA1 and medial perforant path, and lower levels in lateral perforant path, but these were not significant at individual current levels. **(B)** The empirical mean EPSP is plotted as a function of mean FV slope for each level of current. In the CA1 region we found strong evidence of an interaction between injury and FV slope [$F(2, 428) = 6.95$, $p = 0.001$], indicating the presence of an injury effect that differed as a function of FV slope. These results suggest that for a given input (FV) in area CA1, there is a greater output (EPSP) post injury. The results for this interaction for medial perforant path (mPP) did not achieve statistical significance [$F(2, 437) = 2.28$, $p = 0.10$] and there was no evidence of an effect of injury by FV slope interaction in the lateral perforant path (lPP) [$F(2,447) = 0.35$, $p = 0.70$, NS]. There was also no evidence of an overall effect of injury in the lPP [$F(1,6) = 0.023$, $p = 0.89$ NS]. Data presented as animal mean ± standard error of the mean.

which histopathological analysis was performed, this interpretation would be inconsistent with the time course of axonal degeneration previously shown in humans and in this swine model.[18,54]

Our findings suggest that the marked reductions in intra-hippocampal FVs after mild closed-head inertial brain injury may not be explained by axonal loss, but rather reflect a functional

axonal pathology beneath the level of degeneration or overt disconnection. Changes that may underlie the loss of action potential propagation manifesting as fiber-volley attenuation include neurofilament compaction, nodal disruption, and/or alterations in sodium channel kinetics, sub-types or distribution.[55,56] We have previously shown sodium channel disruption in our in vitro model

FIG. 6. Lack of axonal pathology in the hippocampus despite functional alterations. At 7 days after injury or sham conditions, axonal degeneration was assessed both within hippocampal pathways, as well outside the hippocampal structure in sub-cortical white matter tracts (as an internal positive control). Representative micrographs from sham animals are presented in the left column, and from injured animals in the right column. **(A, B)** In sub-cortical white matter, amyloid precursor protein (APP) immunoreactive axons displayed the classic morphological appearance of traumatic axonal injury, including terminally disconnected swollen axonal bulbs, following TBI (A) but were absent in sham animals (B). However, no overt APP accumulation was observed within the hippocampal formation in any animals following injury, including regions that corresponded to the stimulation/recording sites on the contralateral side (i.e., the stratum moleculare layer of the dentate gyrus and the stratum radiatum of the CA1 region) as demonstrated in representative hippocampal sub-fields following sham conditions **(C, E)** or head rotation **(D, F)**. Moreover, neurofilament-200 immunolabeling revealed axons of normal density, morphology and distribution in these regions, with consistent appearance between sham **(G, I)** and injured **(H, J)** animals. Collectively, these observations suggest the functional compromise of intra-hippocampal axons may not be explained by overt axonal loss/degeneration or transport disruption. Scale bar = 25 μM for (A) and (B), 50 μM for (C-J).
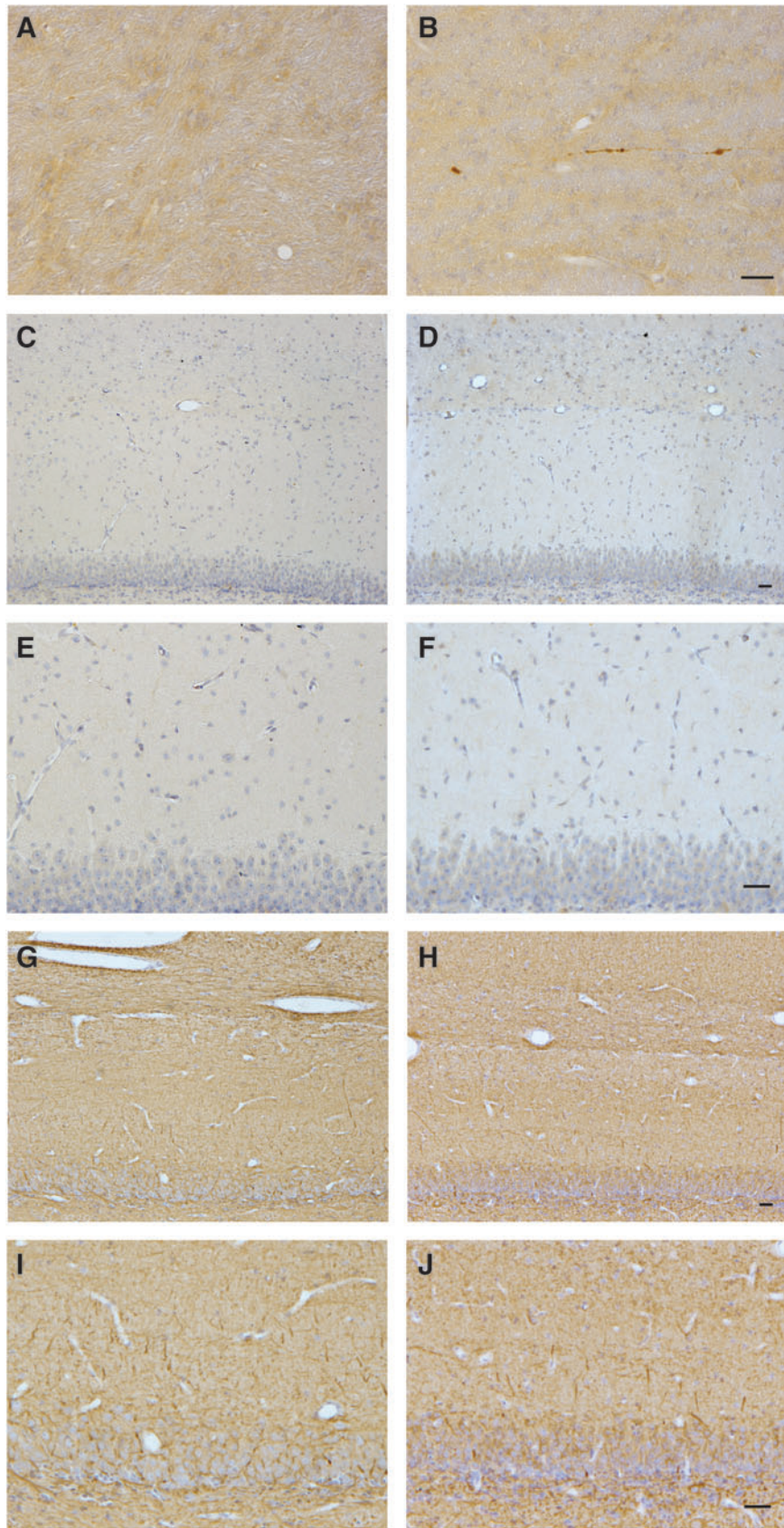
of axonal injury, and the FV reduction may reflect these same mechanisms, or the inefficiency of newly inserted channels.[57–59] Resultant depolarization of the axons could also lead to a decrease in driving force reflected in the lower FV amplitudes. Demyelination or disruption of the nodal architecture also may lead to the same effect on FV; however, overt myelination changes were not detected in this tissue (data not shown).

These functional axonal deficits following mTBI suggest the intriguing possibility that a population of axons is present that is undetected using the current neuropathological standards. Functionally compromised axons in the hippocampus may therefore underlie some aspects of cognitive dysfunction after mTBI.[60] Even minor delays in timing between networks can disrupt important aspects of the oscillatory entrainment of neurons that has been demonstrated in both animal and human cognitive function, and could affect other time relevant synaptic mechanisms, such as spike-timing dependent plasticity.[61–65] Disruptions or delays in the perforant pathway, which projects from the entorhinal cortex and serves as one of the major inputs to the hippocampus, may in particular lead to memory effects, as has been demonstrated in models of Alzheimer's disease.[66–69] Cognitive processing speed after mTBI has been demonstrated as a deficit post-injury, with hippocampal fornix axonal dysfunction suggested as one potential substrate.[43,69–71] Previous efforts to examine electrophysiological changes in FV and action potential propagation have been performed with fluid percussion models in rats and have demonstrated changes post-injury, as well as in some mouse slice experiments[32,33]; however, some of these did not display reduced FVs.[72] Diffuse strain fields from closed-head inertial injury may uniquely induce axonal dysfunction below levels that induce neuronal and axonal degeneration, particularly in specific planes of injury, such as coronal rotation. The level of hippocampal axonal vulnerability may therefore vary based on the plane of head rotation, as has been previously demonstrated in other brain regions in this model.[27]

Synaptic changes in paired pulse ratio

Our data also suggest that synaptic release probabilities were affected following diffuse brain injury, as shown in particular by the loss of paired pulse facilitation in the Schaffer collateral pathway at 7 days post-injury. Paired pulse facilitation is one of the shortest time-scale plasticity measures, usually attributed to residual calcium in the axonal terminals from the previous pulse,[30,73,74] but interpretation of these results are limited by the presence of the population spike in the recordings. While this measure cannot predict the effects on longer-term potentiation and other forms of plasticity, other TBI models have demonstrated changes in LTP in area CA1.[33,50] However, rodent models have seen various effects on paired pulse ratio.[32,50] If release probability has been significantly altered (one interpretation of a decrease in paired pulse ratio), then other forms of plasticity also may be affected, suggesting a potential mechanism for protracted short-term memory problems via disruption of information encoding.

Summary

This is the first report of hippocampal circuitry dysfunction following closed-head diffuse brain injury in a large animal model replicating features of the gyrencephalic neuroanatomy of the human brain. In particular, these data indicate that non-impact inertial TBI in swine leads to axonal dysfunction and changes in synaptic release probability and regional excitability in the hippocampus. Interestingly, we discovered increased EPSPs in response to re-

duced FVs, consistent with an increased release probability or a subtle neurophysiological shift in neuronal excitability and/or synaptic receptor density to account for trauma-induced reductions in axonal function. This adaptive response, presumably to maintain a functional output given a pathologically reduced input, was not revealed by standard analyses of I/O relationships. These neurophysiological changes occurred independent of detectable intra-hippocampal neuronal or axonal degeneration, suggesting that the observed functional shifts occurred directly due to trauma rather than being a consequence of neuronal and/or axonal degeneration.

While it is premature to suggest that these reported hippocampal disruptions lead directly to cognitive dysfunction, significant disruption to hippocampal circuitry is a potential contributor to post-traumatic amnesia and other lingering cognitive deficits following TBI. These findings suggest that this swine model of closed-head diffuse brain injury may be a useful pre-clinical model to study neurophysiological and functional consequences of TBI in humans. Moreover, if future *in vivo* studies establish that the observed post-TBI hyperexcitability changes remain elevated over time, this model also may be useful to investigate post-traumatic hippocampal epileptogenesis. The current findings suggest future studies examining the potential trauma-specific mechanisms underlying hippocampal dysfunction following concussion, a crucial step in identifying therapeutic targets.

Author Disclosure Statement

No competing financial interests exist.

References

1. Coronado, V.G., McGuire, L.C., Sarmiento, K., Bell, J., Lionbarger, M.R., Jones, C.D., Geller, A.I., Khoury, N., and Xu, L. (2012). Trends in traumatic brain injury in the U.S. and the public health response: 1995–2009. J. Safety Res. 43, 299–307.
2. Graham, R., Rivara, F.P., Ford, M.A., and Spicer, C.M. (2014). *Sports-Related Concussions in Youth: Improving the Science, Changing the Culture.* The National Academies Press: Washington, D.C.
3. Jordan, B.D. (2013). The clinical spectrum of sport-related traumatic brain injury. Nature reviews. Neurology 9, 222–230.
4. Hoge, C.W., McGurk, D., Thomas, J.L., Cox, A.L., Engel, C.C., and Castro, C.A. (2008). Mild traumatic brain injury in U.S. soldiers returning from Iraq. N. Engl. J. Med. 358, 453–463.
5. Caruso, D.X. and Levin, H.S. (1992). Cognitive impairment following closed head injury. Neurol. Clin. 10, 879–893.
6. Ryan, L.M. and Warden, D.L. (2003). Post concussion syndrome. Int. Rev. Psychiatry 15, 310–316.
7. Monti, J.M., Voss, M.W., Pence, A., McAuley, E., Kramer, A.F., and Cohen, N.J. (2013). History of mild traumatic brain injury is associated with deficits in relational memory, reduced hippocampal volume, and less neural activity later in life. Front. Aging Neurosci. 5, 41.

8. Browne, K.D., Chen, X.H., Meaney, D.F., and Smith, D.H. (2011). Mild traumatic brain injury and diffuse axonal injury in swine. J. Neurotrauma 28, 1747–1755.

9. Blumbergs, P.C., Scott, G., Manavis, J., Wainwright, H., Simpson, D.A., and McLean, A.J. (1994). Staining of amyloid precursor protein to study axonal damage in mild head injury. Lancet 344, 1055–1056.

10. Kotapka, M.J., Graham, D.I., Adams, J.H., and Gennarelli, T.A. (1992). Hippocampal pathology in fatal non-missile human head injury. Acta Neuropathol. 83, 530–534.

11. Maxwell, W.L., Dhillon, K., Harper, L., Espin, J., MacIntosh, T.K., Smith, D.H., and Graham, D.I. (2003). There is differential loss of pyramidal cells from the human hippocampus with survival after blunt head injury. J. Neuropathol. Exp. Neurol. 62, 272–279.

12. Gibson, K.L., Remson, L., Smith, A., Satterlee, N., Strain, G.M., and Daniloff, J.K. (1991). Comparison of nerve regeneration through different types of neural prostheses. Microsurgery 12, 80–85.

13. Hicks, R.R., Smith, D.H., Lowenstein, D.H., Saint Marie, R., and McIntosh, T.K. (1993). Mild experimental brain injury in the rat induces cognitive deficits associated with regional neuronal loss in the hippocampus. J. Neurotrauma 10, 405–414.

14. Christidi, F., Bigler, E.D., McCauley, S.R., Schnelle, K.P., Merkley, T.L., Mors, M.B., Li, X., Macleod, M., Chu, Z., Hunter, J.V., Levin, H.S., Clifton, G.L., and Wilde, E.A. (2011). Diffusion tensor imaging of the perforant pathway zone and its relation to memory function in patients with severe traumatic brain injury. J. Neurotrauma 28, 711–725.

15. Bigler, E.D., Blatter, D.D., Anderson, C.V., Johnson, S.C., Gale, S.D., Hopkins, R.O., and Burnett, B. (1997). Hippocampal volume in normal aging and traumatic brain injury. A.J.N.R. Am. J. Neuroradiol. 18, 11–23.

16. Lowenstein, D.H., Thomas, M.J., Smith, D.H., and McIntosh, T.K. (1992). Selective vulnerability of dentate hilar neurons following traumatic brain injury: a potential mechanistic link between head trauma and disorders of the hippocampus. J. Neurosci. 12, 4846–4853.

17. Meaney, D.F., Smith, D.H., Shreiber, D.I., Bain, A.C., Miller, R.T., Ross, D.T., and Gennarelli, T.A. (1995). Biomechanical analysis of experimental diffuse axonal injury. J. Neurotrauma 12, 689–694.

18. Smith, D.H., Chen, X.H., Xu, B.N., McIntosh, T.K., Gennarelli, T.A., and Meaney, D.F. (1997). Characterization of diffuse axonal pathology and selective hippocampal damage following inertial brain trauma in the pig. J. Neuropathol. Exp. Neurol. 56, 822–834.

19. Cullen, D.K., Harris, J.P., Browne, K.D., Wolf, J.A., Duda, J.E., Meaney, D.F., Margulies, S.S., and Smith, D.H. (2016). A porcine model of traumatic brain injury via head rotational acceleration, in: Injury Models of Central Nervous System: Traumatic Brain Injury, Methods in Molecular Biology. Humana Press: New York.

20. Morris, M.D. (2011). Design of Experiments: An Introduction Based on Linear Models. CRC Press, Chapman & Hall, Boca Raton, FL.

21. R Core Team (2015). R: A language and environment for statistical computing. Available at: https://cran.r-project.org/doc/manuals/fullrefman.pdf. Accessed March 31, 2017.

22. Johnson, V.E., Stewart, J.E., Begbie, F.D., Trojanowski, J.Q., Smith, D.H., and Stewart, W. (2013). Inflammation and white matter degeneration persist for years after a single traumatic brain injury. Brain 136, 28–42.

23. Sherriff, F.E., Bridges, L.R., and Sivaloganathan, S. (1994). Early detection of axonal injury after human head trauma using immunocytochemistry for beta-amyloid precursor protein. Acta Neuropathol. (Berl.) 87, 55–62.

24. Gentleman, S.M., Nash, M.J., Sweeting, C.J., Graham, D.I., and Roberts, G.W. (1993). Beta-amyloid precursor protein (beta APP) as a marker for axonal injury after head injury. Neurosci. Lett. 160, 139–144.

25. Gentleman, S.M., Roberts, G.W., Gennarelli, T.A., Maxwell, W.L., Adams, J.H., Kerr, S., and Graham, D.I. (1995). Axonal injury: a universal consequence of fatal closed head injury? Acta Neuropathol. 89, 537–543.

26. Trojanowski, J.Q., Walkenstein, N., and Lee, V.M. (1986). Expression of neurofilament subunits in neurons of the central and peripheral nervous system: an immunohistochemical study with monoclonal antibodies. J. Neurosci. 6, 650–660.

27. Smith, D.H., Nonaka, M., Miller, R., Leoni, M., Chen, X.H., Alsop, D., and Meaney, D.F. (2000). Immediate coma following inertial brain injury dependent on axonal damage in the brainstem. J. Neurosurg. 93, 315–322.

28. Browne, K.D., Chen, X.H., Meaney, D.F., and Smith, D.H. (2011). Mild traumatic brain injury and diffuse axonal injury in swine. J. Neurotrauma 28, 1747–1755.

29. Eucker, S.A., Smith, C., Ralston, J., Friess, S.H., and Margulies, S.S. (2011). Physiological and histopathological responses following closed rotational head injury depend on direction of head motion. Exp. Neurol. 227, 79–88.

30. Creager, R., Dunwiddie, T., and Lynch, G. (1980). Paired-pulse and frequency facilitation in the CA1 region of the in vitro rat hippocampus. J. Physiol. 299, 409–424.

31. McNaughton, B.L. (1980). Evidence for two physiologically distinct perforant pathways to the fascia dentata. Brain Res. 199, 1–19.

32. Reeves, T.M., Kao, C.Q., Phillips, L.L., Bullock, M.R., and Povlishock, J.T. (2000). Presynaptic excitability changes following traumatic brain injury in the rat. J. Neurosci. Res. 60, 370–379.

33. Norris, C.M. and Scheff, S.W. (2009). Recovery of afferent function and synaptic strength in hippocampal CA1 following traumatic brain injury. J. Neurotrauma 26, 2269–2278.

34. Smith, C.J., Xiong, G., Elkind, J.A., Putnam, B., and Cohen, A.S. (2015). Brain injury impairs working memory and prefrontal circuit function. Front. Neurol. 6, 240.

35. Johnson, V.E., Stewart, W., and Smith, D.H. (2012). Axonal pathology in traumatic brain injury. Exp Neurol. 246, 35–43.

36. Smith, D.H. and Meaney, D.F. (2000). Axonal damage in traumatic brain injury. Neuroscientist 6, 483–495.

37. Ommaya, A.K. and Gennarelli, T.A. (1974). Cerebral concussion and traumatic unconsciousness. Correlation of experimental and clinical observations of blunt head injuries. Brain 97, 633–654.

38. Adams, J.H., Doyle, D., Ford, I., Gennarelli, T.A., Graham, D.I., and McClellan, D.R. (1989). Diffuse axonal injury in head injury: definition, diagnosis, and grading. Histopathology 15, 49–59.

39. Povlishock, J.T. (1992). Traumatically induced axonal injury: pathogenesis and pathobiological implications. Brain Pathol. 2, 1–12.

40. Langlois, J.A., Rutland-Brown, W., and Wald, M.M. (2006). The epidemiology and impact of traumatic brain injury: a brief overview. J. Head Trauma Rehabil. 21, 375–378.

41. Vanderploeg, R.D., Crowell, T.A., and Curtiss, G. (2001). Verbal learning and memory deficits in traumatic brain injury: encoding, consolidation, and retrieval. J. Clin. Exp. Neuropsychol. 23, 185–195.

42. De Kruijk, J.R., Twijnstra, A., and Leffers, P. (2001). Diagnostic criteria and differential diagnosis of mild traumatic brain injury. Brain Inj. 15, 99–106.

43. De Monte, V.E., Geffen, G.M., and Massavelli, B.M. (2006). The effects of post-traumatic amnesia on information processing following mild traumatic brain injury. Brain Inj. 20, 1345–1354.

44. Leininger, B.E., Gramling, S.E., Farrell, A.D., Kreutzer, J.S., and Peck, E.A. (1990). Neuropsychological deficits in symptomatic minor head injury patients after concussion and mild concussion. J. Neurol. Neurosurg. Psychiatry 53, 293–296.

45. Santhakumar, V., Ratzliff, A.D., Jeng, J., Toth, Z., and Soltesz, I. (2001). Long-term hyperexcitability in the hippocampus after experimental head trauma. Ann. Neurol. 50, 708–717.

46. Golarai, G., Greenwood, A.C., Feeney, D.M., and Connor, J.A. (2001). Physiological and structural evidence for hippocampal involvement in persistent seizure susceptibility after traumatic brain injury. J. Neurosci. 21, 8523–8537.

47. Hanell, A., Greer, J., and Jacobs, K. (2015). Increased network excitability due to altered synaptic inputs to neocortical layer V intact and axotomized pyramidal neurons after mild traumatic brain injury. J. Neurotrauma 32, 1590–1598.

48. Turrigiano, G.G. (1999). Homeostatic plasticity in neuronal networks: the more things change, the more they stay the same. Trends Neurosci. 22, 221–227.

49. Dinocourt, C., Aungst, S., Yang, K., and Thompson, S.M. (2011). Homeostatic increase in excitability in area CA1 after Schaffer collateral transection in vivo. Epilepsia 52, 1656–1665.

50. Schwarzbach, E., Bonislawski, D.P., Xiong, G., and Cohen, A.S. (2006). Mechanisms underlying the inability to induce area CA1 LTP in the mouse after traumatic brain injury. Hippocampus 16, 541–550.

51. Witgen, B.M., Lifshitz, J., Smith, M.L., Schwarzbach, E., Liang, S.L., Grady, M.S., and Cohen, A.S. (2005). Regional hippocampal alteration associated with cognitive deficit following experimental brain injury: a systems, network and cellular evaluation. Neuroscience 133, 1–15.

52. Griesemer, D. and Mautes, A.M. (2007). Closed head injury causes hyperexcitability in rat hippocampal CA1 but not in CA3 pyramidal cells. J. Neurotrauma 24, 1823–1832.

53. Gennarelli, T.A., Thibault, L.E., Adams, J.H., Graham, D.I., Thompson, C.J., and Marcincin, R.P. (1982). Diffuse axonal injury and traumatic coma in the primate. Ann. Neurol. 12, 564–574.

54. Blumbergs, P.C., Jones, N.R., and North, J.B. (1989). Diffuse axonal injury in head trauma. J. Neurol. Neurosurg. Psychiatry 52, 838–841.

55. Stone, J.R., Singleton, R.H., and Povlishock, J.T. (2001). Intra-axonal neurofilament compaction does not evoke local axonal swelling in all traumatically injured axons. Exp. Neurol. 172, 320–331.

56. Johnson, V.E., Stewart, W., Weber, M.T., Cullen, D.K., Siman, R., and Smith, D.H. (2016). SNTF immunostaining reveals previously undetected axonal pathology in traumatic brain injury. Acta Neuropathol. 131, 115–135.

57. Wolf, J.A., Stys, P.K., Lusardi, T., Meaney, D., and Smith, D.H. (2001). Traumatic axonal injury induces calcium influx modulated by tetrodotoxin-sensitive sodium channels. J. Neurosci. 21, 1923–1930.

58. Iwata, A., Stys, P.K., Wolf, J.A., Chen, X.H., Taylor, A.G., Meaney, D.F., and Smith, D.H. (2004). Traumatic axonal injury induces proteolytic cleavage of the voltage-gated sodium channels modulated by tetrodotoxin and protease inhibitors. J. Neurosci. 24, 4605–4613.

59. Yuen, T.J., Browne, K.D., Iwata, A., and Smith, D.H. (2009). Sodium channelopathy induced by mild axonal trauma worsens outcome after a repeat injury. J. Neurosci. Res. 87, 3620–3625.

60. Wolf, J.A. and Koch, P.F. (2016). Disruption of network synchrony and cognitive dysfunction after traumatic brain injury. Front. Syst. Neurosci. 10, 43.

61. Pajevic, S., Basser, P.J., and Douglas Fields, R. (2013). Role of myelin plasticity in oscillations and synchrony of neuronal activity. Neuroscience 276, 135–147.

62. Rutishauser, U., Ross, I.B., Mamelak, A.N., and Schuman, E.M. (2010). Human memory strength is predicted by theta-frequency phase-locking of single neurons. Nature 464, 903–907.

63. Maurer, A.P. and McNaughton, B.L. (2007). Network and intrinsic cellular mechanisms underlying theta phase precession of hippocampal neurons. Trends Neurosci. 30, 325–333.

64. Lee, D., Gurkoff, G., Izadi, A., Berman, R., Ekstrom, A., Muizelaar, J., Lyeth, B., and Shahlaie, K. (2013). Medial septal nucleus theta frequency deep brain stimulation improves spatial working memory after traumatic brain injury. J. Neurotrauma 30, 131–139.

65. Akam, T. and Kullmann, D.M. (2014). Oscillatory multiplexing of population codes for selective communication in the mammalian brain. Nat. Rev. Neurosci. 15, 111–122.

66. Braak, H. and Braak, E. (1992). The human entorhinal cortex: normal morphology and lamina-specific pathology in various diseases. Neurosci. Res. 15, 6–31.

67. Hyman, B.T., Van Hoesen, G.W., Kromer, L.J., and Damasio, A.R. (1986). Perforant pathway changes and the memory impairment of Alzheimer's disease. Ann Neurol 20, 472–481.

68. Kirkby, D.L. and Higgins, G.A. (1998). Characterization of perforant path lesions in rodent models of memory and attention. Eur. J. Neurosci. 10, 823–838.

69. Fisher, D.C., Ledbetter, M.F., Cohen, N.J., Marmor, D., and Tulsky, D.S. (2000). WAIS-III and WMS-III profiles of mildly to severely brain-injured patients. Appl. Neuropsychol. 7, 126–132.

70. Mathias, J.L., Beall, J.A., and Bigler, E.D. (2004). Neuropsychological and information processing deficits following mild traumatic brain injury. J. Int. Neuropsychol. Soc.10, 286–297.

71. Yallampalli, R., Wilde, E.A., Bigler, E.D., McCauley, S.R., Hanten, G., Troyanskaya, M., Hunter, J.V., Chu, Z., Li, X., and Levin, H.S. (2013). Acute white matter differences in the fornix following mild traumatic brain injury using diffusion tensor imaging. J. Neuroimaging 23, 224–227.

72. Cole, J.T., Mitala, C.M., Kundu, S., Verma, A., Elkind, J.A., Nissim, I., and Cohen, A.S. (2010). Dietary branched chain amino acids ameliorate injury-induced cognitive impairment. Proc. Natl. Acad. Sci. 107, 366–371.

73. Lomo, T. (1971). Potentiation of monosynaptic EPSPs in the perforant path-dentate granule cell synapse. Exp. Brain. Res. 12, 46–63.

74. Zucker, R.S. (1989). Short-term synaptic plasticity. Ann. Rev. Neurosci. 12, 13–31.

Address correspondence to:
D. Kacy Cullen, PhD
Department of Neurosurgery
University of Pennsylvania
Room 105 Hayden Hall
3320 Smith Walk
Philadelphia, PA 19104

E-mail: dkacy@mail.med.upenn.edu